SUPPLEMENTAL FIGURES AND TABLES

S16 throws a conformational switch during assembly of 30S 5' domain

Priya Ramaswamy[1] and Sarah A. Woodson[2]
[1]Program in Cell, Molecular and Developmental Biology and Biophysics and [2]T. C. Jenkins Department of Biophysics, Johns Hopkins University, 3400 N. Charles St., Baltimore, MD 21218 USA

SUPPLEMENTARY FIG. 1

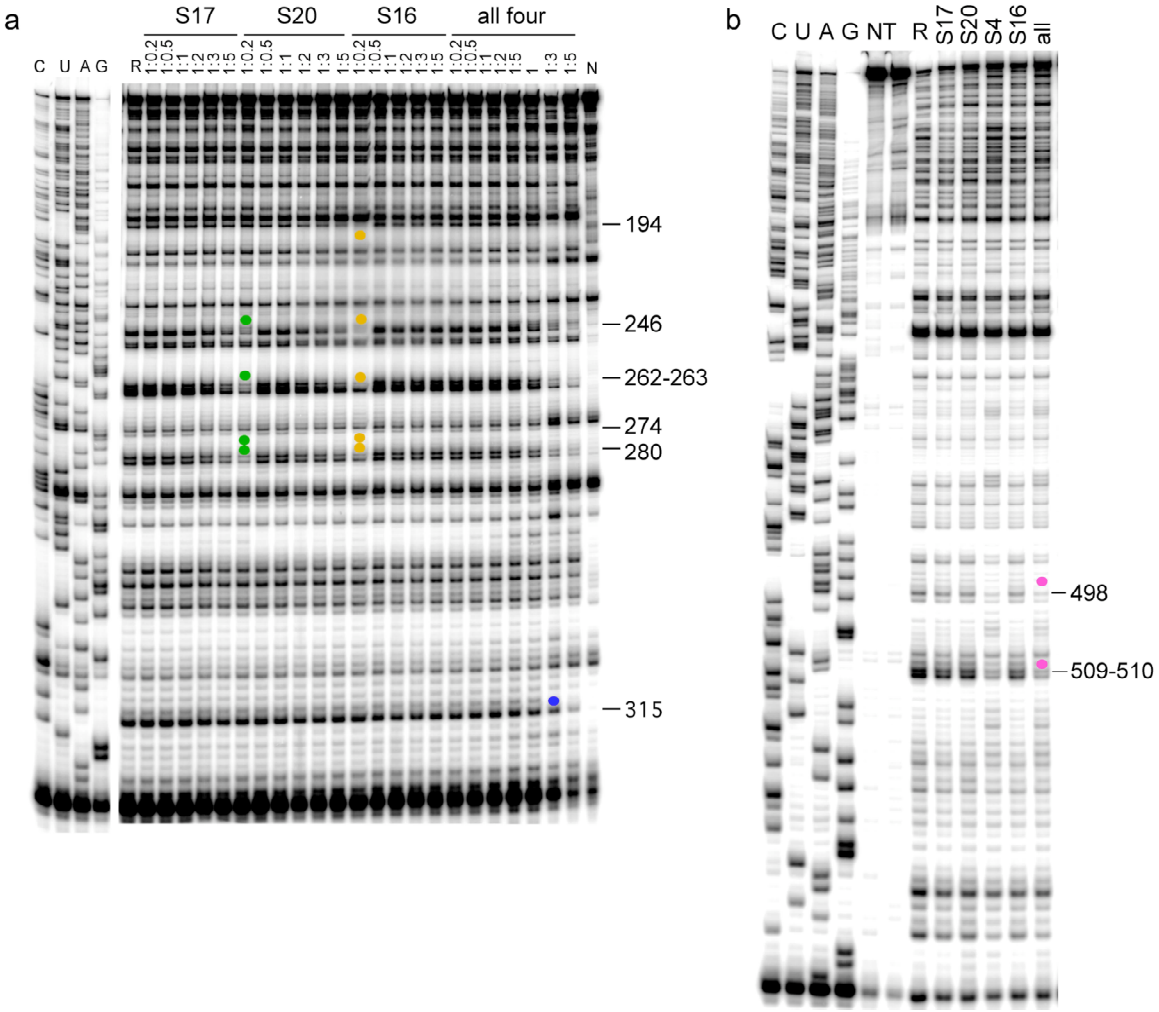

Supplementary Fig. 1. Verification of protein contacts by DMS footprinting. The 16S 5' domain was coincubated with S4, S16, S17, or S20, or all four proteins, for 1 hour at 42°C. Samples were modified as described in Methods and analyzed by primer extension. **(a)** Primer annealing at 16S nt 323. Predicted protein contacts [1] are shown to the right and with colored dots. Lanes NT, no treatment; R, RNA only; C, U, A, G, sequence ladder. Green circles, S17; yellow circles, S20; blue circle, S16. **(b)** Primer annealing at 16S nt 560, showing S4 contacts (pink).

SUPPLEMENTARY FIG. 2

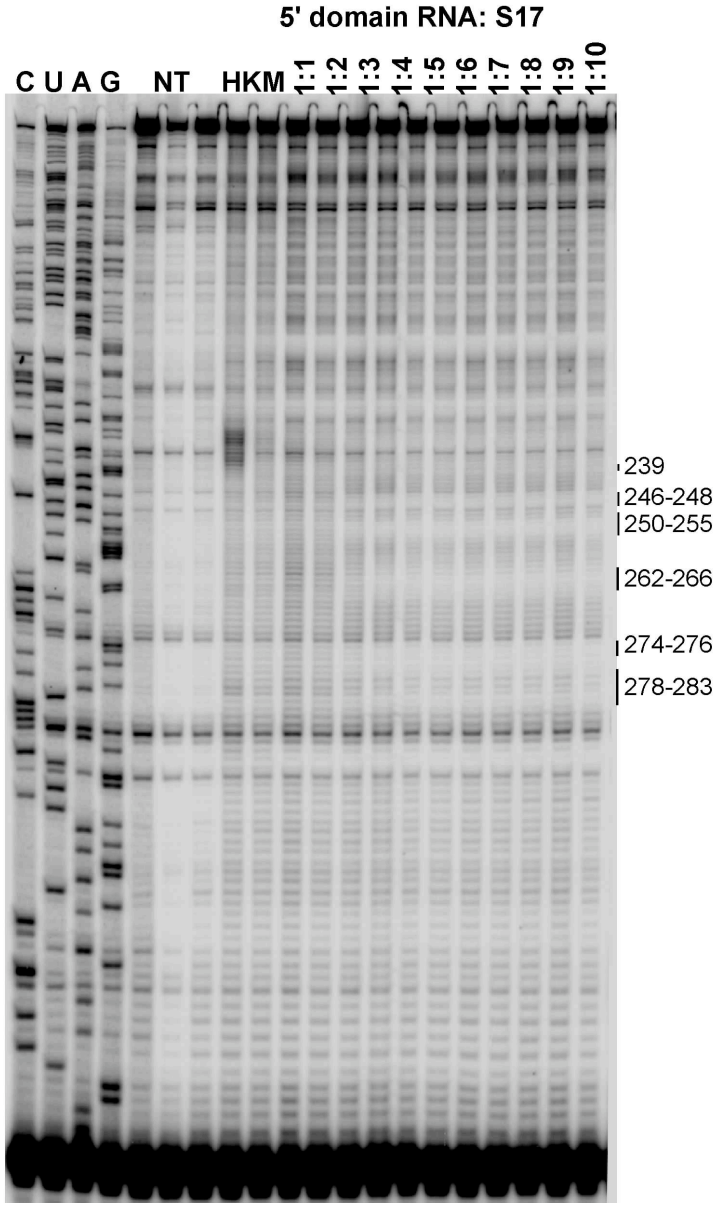

Supplementary Fig. 2. Saturation of RNA backbone contacts. The 16S 5' domain was prefolded for 15-20 minutes and coincubated with protein for 40 minutes. The molar ratio of protein to RNA was varied from 1:1 to 1:10. A sample titration for S17 (primer 323) is shown. Similar titrations were carried out for S4, S16, and S20. Lane NT, no treatment; H, RNA only in 80 mM K^+Hepes; K, RNA only in 80 mM K^+Hepes plus 330 mM KCl; M, RNA only in reconstitution buffer (20 mM $MgCl_2$); C, U, A, G, sequence ladders. Predicted S17 contacts are shown to the right and are based on the crystal structures of the *E. coli* 30S subunit [2-4].

SUPPLEMENTARY FIG. 3

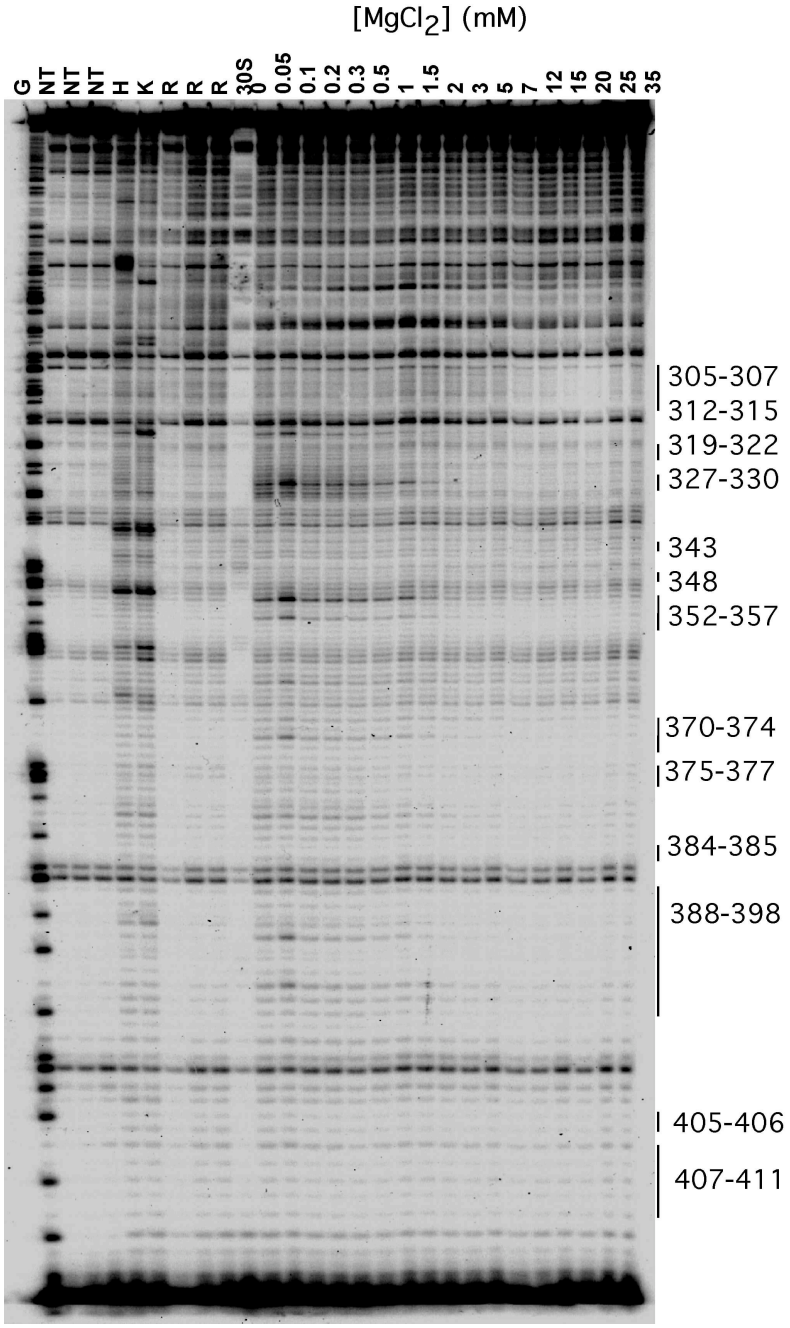

Supplementary Fig. 3. Equilibrium Fe(II)EDTA hydroxyl radical footprinting of the 5' domain. The 16S 5' domain (nt 21-562) was pre-folded for 20 minutes at 37°C in 0-35 mM $MgCl_2$. **(a,b)** Assembly proteins S4, S16, S17, and S20 and RNA were coincubated for another 40 minutes. Samples were treated and analyzed as described in Methods. Lanes, as described in Figure S2. R, RNA only in reconstitution buffer. To the right are predicted protections due to RNA-RNA contacts based on the crystal structure of the

SUPPLEMENTARY FIG. 3, cont.

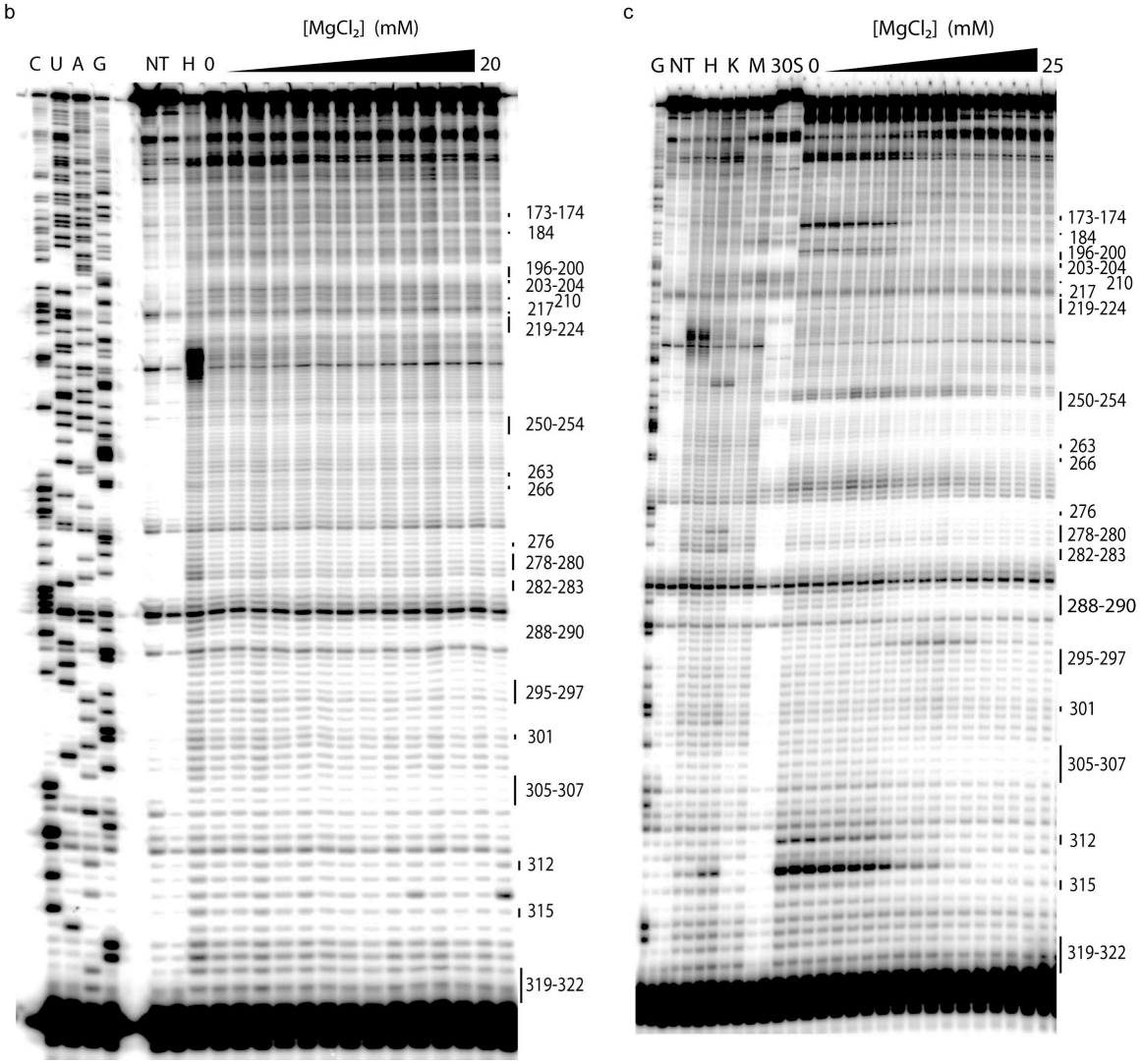

Legend to Supplementary Fig. 3, cont.
E.coli 30S ribosome [4]. **(b)** Further data for a different region of the RNA alone (primer 323). Data were analyzed as in Fig. 2. **(c)** Data for region 323 on the RNA plus proteins S4,S17 and S20.

SUPPLEMENTARY FIG. 4

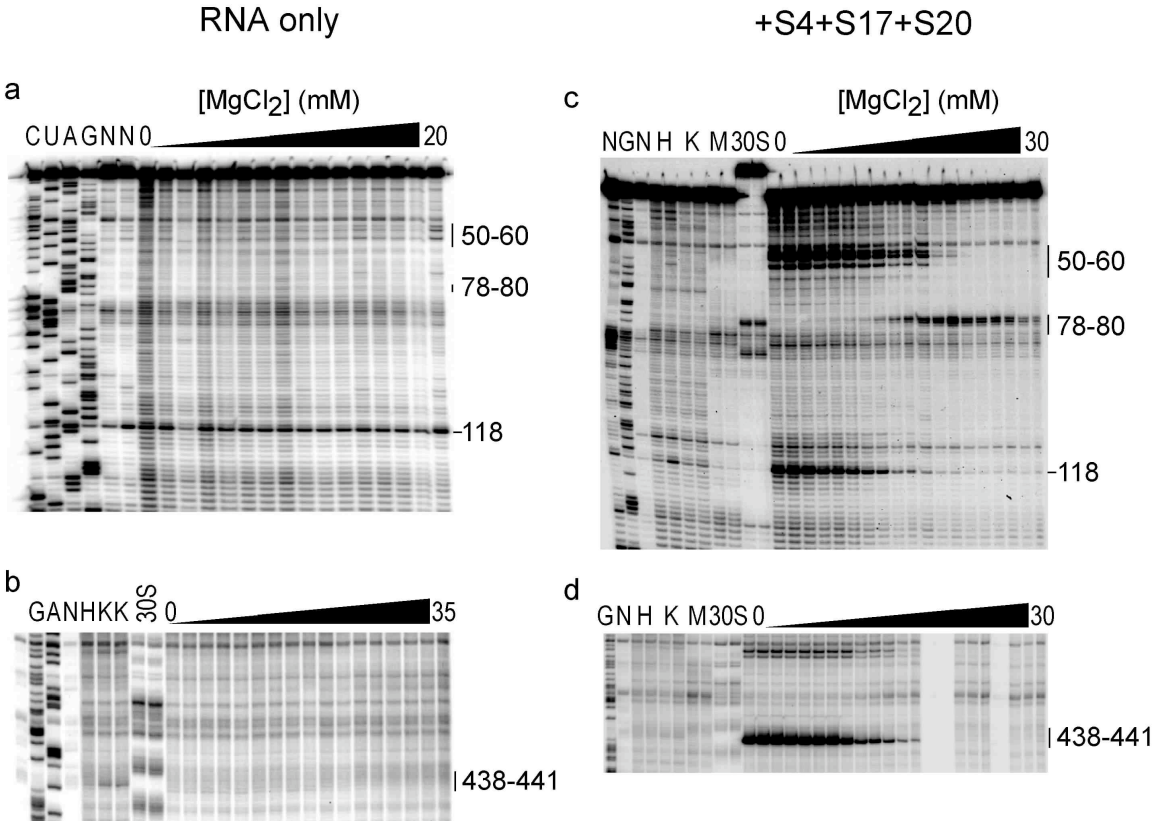

Supplementary Fig. 4. Enhanced cleavage in the presence of S4 + S17 + S20. Data for additional 5' domain residues with enhanced hydroxyl radical cleavage in KCl in the presence of proteins. See Fig. 4 for further information. **(a,b)** RNA only, folded in 0 – 20 mM $MgCl_2$ (top). lanes C, U, G,A, sequencing ladders, N, no Fe(II)-EDTA treatment, H, 80 mM Hepes, K, + 330 mM KCl, 30S, native 30S complexes in 20 mM $MgCl_2$. **(c,d)** RNA plus proteins S4, S17, and S20. Labels as above.

SUPPLEMENTARY FIG. 5

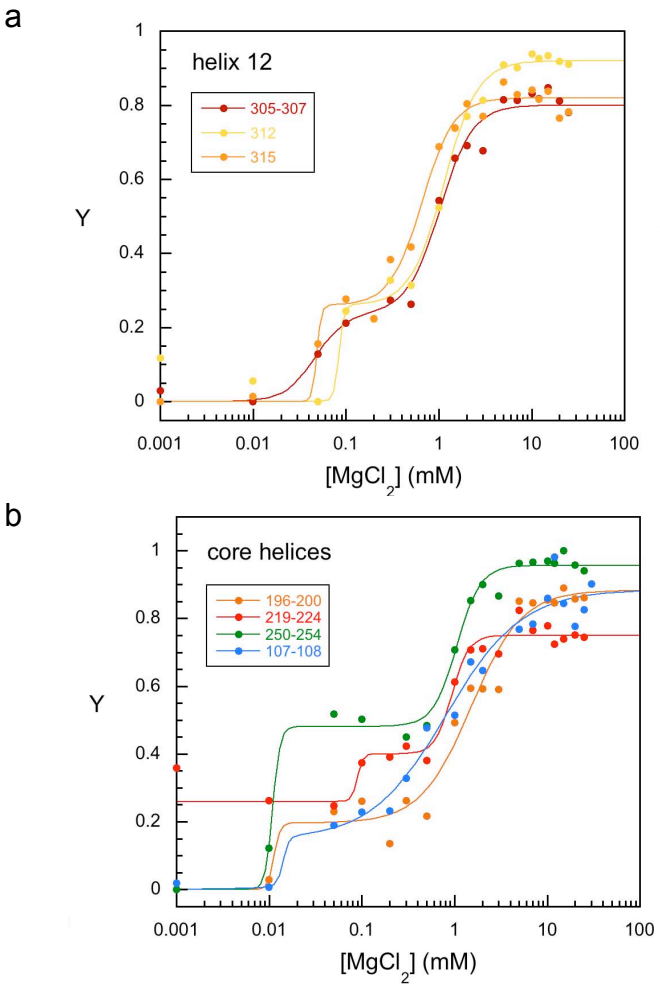

Supplementary Fig. 5. Protection of selected 5' domain nucleotides in the presence of S4 + S17 + S20. Data for individual residues are shown as indicated in each key. **(a)** Additional data for the base of helix 12. **(b)** Protection of core helices. Core helices are H10 (nt 196-200), H7 (nt 219-224), H11 (nt 250-254) and H6a (nt 107-108). The change in relative saturation (Y) vs. [$MgCl_2$] was fit to two sequential cooperative two-state transitions or a cooperative four-state model, as described in Methods. Each protected region was normalized to the maximum extent of cleavage (Y=0), and the extent of cleavage in 30S ribosomes (Y=1), which was at or near the minimum intensity.

SUPPLEMENTARY FIG. 6

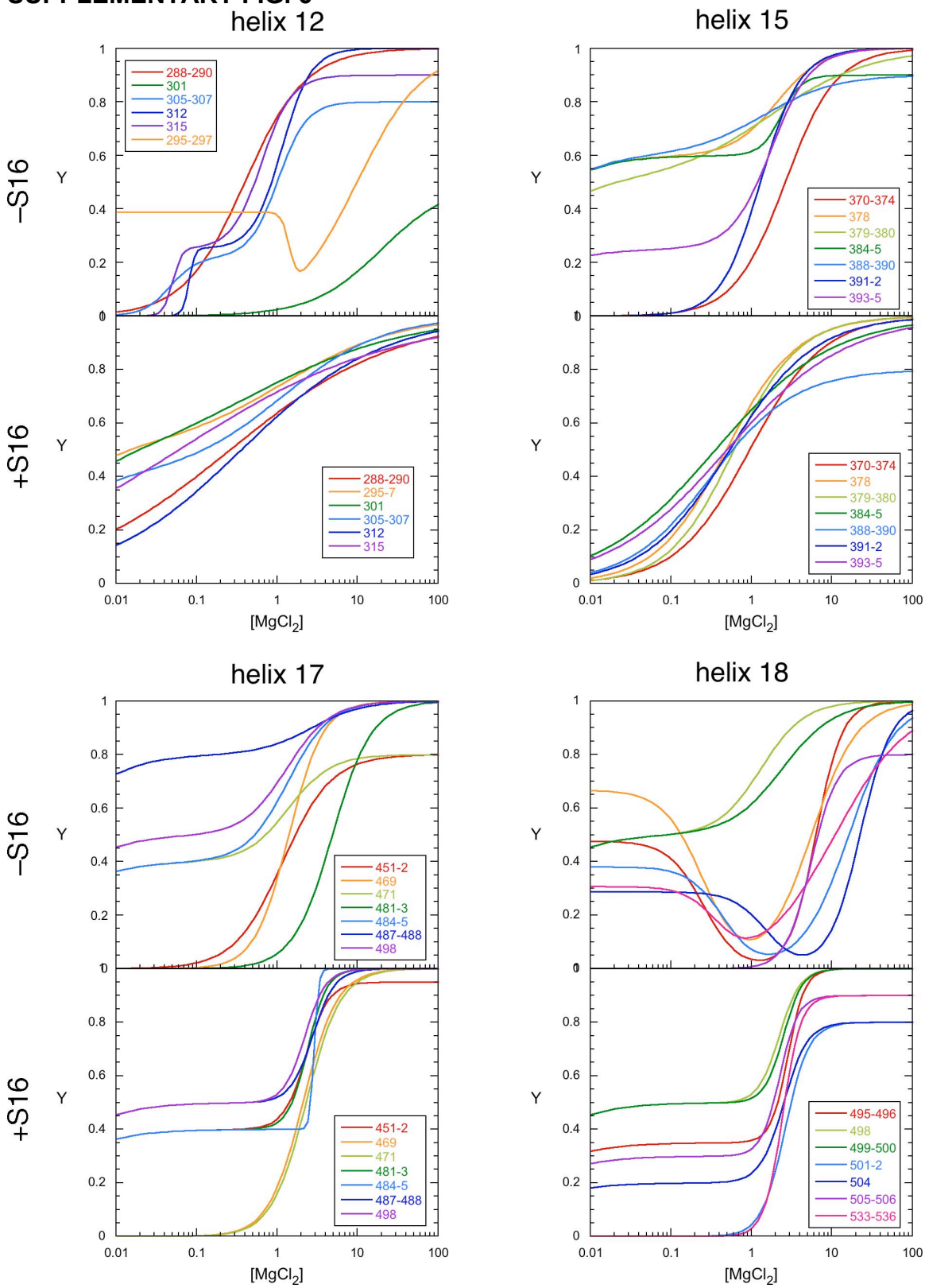

Supplementary Fig. 6. Alignment of Mg^{2+}-dependent transitions in the presence and absence of S16. Backbone protection of residues in individual helices are superimposed, as indicated in the keys to each plot. –S16, titrations in the presence of S4, S17 and S20; +S16, titrations in the presence of S4, S17, S16 and S20. For clarity, only the fitted curves are shown. Parameters for individual fits are given in Supplemental Table 1, and the data illustrated in Fig. 5 and Fig. S4. Lower baselines (+S16) in helices 17 and 18 are uncertain due to strong cleavage of the unfolded RNA control in these experiments.

SUPPLEMENTARY FIG. 7

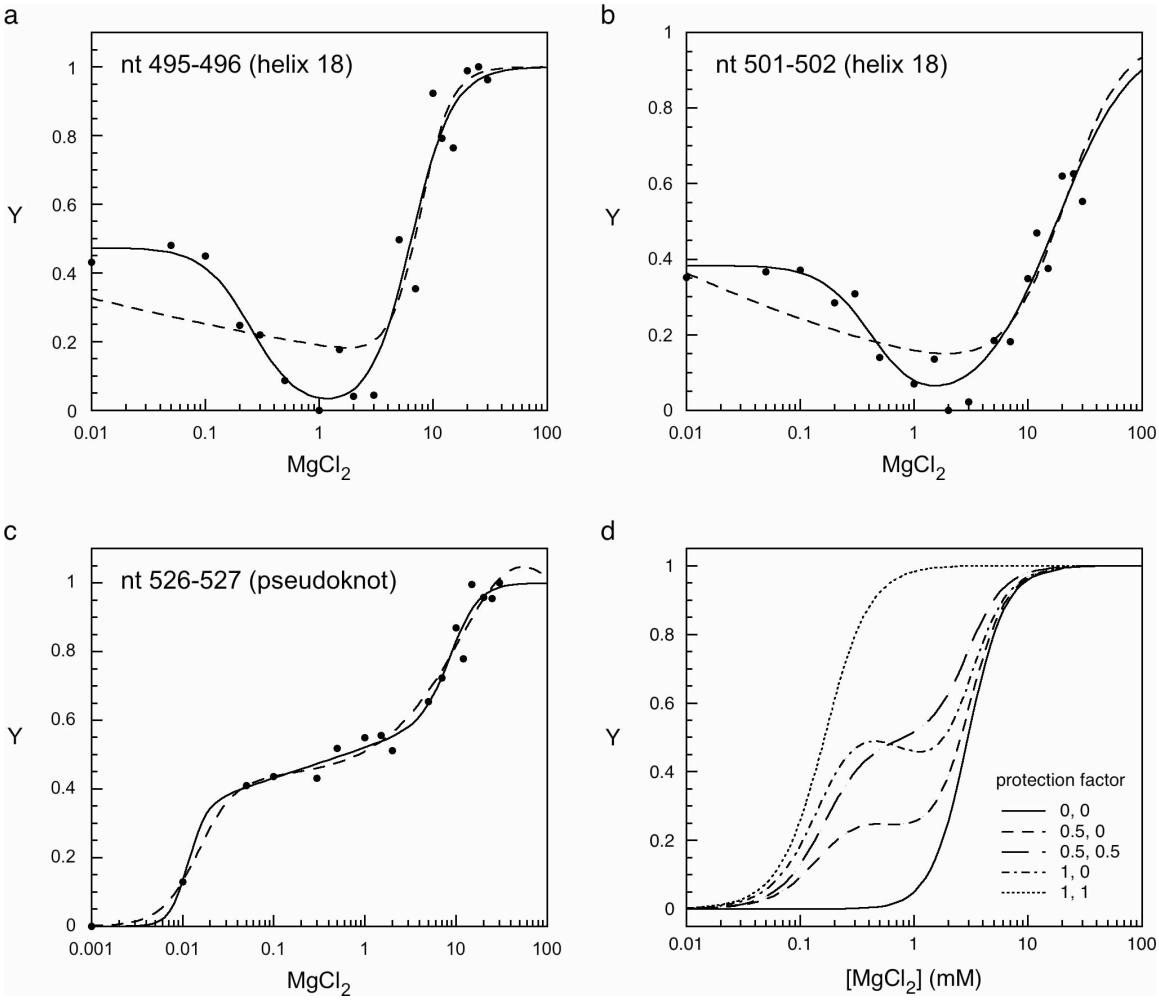

Supplementary Fig. 7. Comparison of three- and four-state models. (a-c) The relative saturation (Y) of residues in helix 18 individual helices was fit to either a four-state model (solid line) or three-state model (dashed line). The four-state model assumes two I states, one in which the residue is protected and the other in which it is cleaved. The three-state model assumes a single I state that is partially protected. While the three-state model can explain a plateau in the titration curves (eg, nt 526-527), it does not adequately fit the transient reexposure of the RNA backbone (eg, nt 495-496 and 501-502). **(d)** Simulated curves for the four-state model, illustrating the effect of the backbone protection in intermediate states. In each case, the initial state (U) is unprotected (p = 0), the native state (N) is fully protected (p = 1). For each curve, the two intermediates were assigned the protection values given in the legend.

Supplementary Table 1: Mg^{2+}-dependent formation of 5' domain tertiary interactions by hydroxyl radical footprinting[a]

(a) RNA only

nts	C_m, 1	n, 1	amp 1	C_m, 2	n, 2	amp 2
59-65	1.1	1.0	50%			
66-72	3.9	0.96	30%			
100-105	5.5	1.1	30%			
107-108	2.3	1.2	30%			
110-114	0.84	0.92	40%			
115-116	0.45	1.6	60%			
119	0.27	2.4	60%			
121-124	0.22	1.6	60%			
131-133	≥ 20	--	45%			
134-135	0.52	1.3	50%			
142-143	≥ 20	--	nd			
151-153	7.5	1.9	75%			
173-174						
184	≥ 20	--	25%			
196-200	≥ 20	--	30%			
203-204	≥ 20	--	nd			
210	≥ 20	--	20%			
217	≥ 20	--	20%			
219-224	≥ 20	--	20%			
250-254	≥ 20	--	20%			
263	≥ 20	--	20%			
266	≥ 20	--	20%			
276	≥ 20	--	20%			
278-280	≤ 0.01[d]	--	60%			
282-283	≥ 20	--	20%			
288-290	1.3	1.7	75%			
295-297	≥ 20	--	30%			
301	≥ 20	--	40%			
305-307	≥ 20	--	30%			
312	≥ 20	--	30%			
315	≥ 20	--	40%			
319-322	≥ 20	--	20%			
327-330	18	0.91	100%			
343	≥ 20	--	50%			
348	0.2	1.4	30%	14	6.4	20%
352-357	0.4	1.5	30%	18	5.6	20%
364	≥ 20	--	40%			
370-374	0.36	5.1	20%	17	1.1	40%
378	0.3	10	15%	9.3	3.2	55%
379-380	0.38	2.9	20%	8.8	4.1	50%

nts	C_m, 1	n, 1	amp 1	C_m, 2	n, 2	amp 2
384-385	0.15	2.5	15%	46	1.3	30%
388-390	0.29	4.2	25%	9.2	3.4	35%
391-392	≤ 0.01	--	50%	4.1	1.0	50%
393-395	≤ 0.01	--	40%	0.71	1.0	60%
398-399	0.3	4.6	40%	21	2.7	40%
405-406	≥ 20	--	40%			
427-429	≥ 20	--	20%			
451-452	≥ 20	--	20%			
469	3.1	2.4	60%			
471	≥ 20	--	20%			
481-483	≥ 20	--	20%			
484-485	≥ 20	--	40%			
487-488	≤ 0.01	--	60%			
495-496	≤ 0.01	--	30%	9.7	4.6	30%
498	≤ 0.01	--	70%			
499-500	≤ 0.01	--	60%			
501-502	≥ 20	--	30%			
504	≥ 20	--	30%			
505-506	≥ 20	--	30%			
513	≥ 20	--	40%			
516-518	≥ 20	--	40%			
521-522	0.61	1.2	100%			
524-527	0.26	1.3	80%			
528-531	0.38	0.65	75%			
533-536	≥ 20	--	20%			

[a]Midpoints (C_m) and Hill coefficients (n_H) were obtained from individual titration curves as described in Methods; parameters for fits to eq. 2 are shown. Data for residues (nts) protected by interactions within the 5' domain of the 16S rRNA are shown. Reproducibility between separate trials was typically ± 20% (C_m) or ± 50% (n_H), and less than ± 50% (C_m) or ± 100% (n_H).

[b]nd, not determined.

[c]Unprotected or weakly protected residues for which no Mg^{2+}-dependent transition could be measured were assumed to have $C_m \geq 20$ mM.

[d]Residues protected in salt and no $MgCl_2$ were assumed to have $C_m \leq 0.01$ mM

Suppl. Table 1 (b) RNA plus protein S4, S17, and S20

nts	C_m, 1	n, 1	amp 1	C_m, 2	n, 2	amp 2
59-65	0.80	0.98	100%			
66-72	0.75	1.2	100%			
100-105	1.1	0.75	100%			
107-108	0.03	2.1	20%	0.93	1.3	70%
110-114	0.34	0.7	90%			
115-116	0.24	0.73	100%			
119	0.2	0.85	100%			
121-124	0.22	0.78	85%			
131-133	0.43	1.52	100%			
134-135	0.17	0.89	100%			
142-143	0.41	1.1	100%			
151-153	2.3	2.4	100%			
173-174	0.74	2.1	100%			
184	0.59	1.2	80%			
196-200	0.016	4.0	20%	2.3	1.8	70%
203-204	≥ 20	--				
210						
217	0.11	0.74	80%			
219-224	0.08	7.4	40%	0.93	3.6	40%
250-254	0.012	4.6	50%	1.1	3.5	50%
263	≤ 0.01	--	80%	0.75	1.5	20%
266	≤ 0.01	--	40%	0.75	0.6	40%
276	0.42	0.47	80%			
278-280	≤ 0.01	--	70%	0.45	0.44	20%
282-283	≤ 0.01	--	60%			
288-290	0.4	1.2	100%			
301	≥ 20	--	50%			
305-307	0.047	2.6	22%	1.0	2.5	58%
312	0.08	14.2	25%	1.2	2.4	75%
315	0.05	8.3	25%	0.65	2.3	65%
319-322	0.77	0.6	80%			
327-330	2.0	1.3	100%			
343	0.001	1	90%			
348	0.001	1	90%			
352-357	1.8	1.2	100%			
364	≤ 0.01	--	30%	4.8	1.2	70%
370-374	2.7	1.4	100%			
378	≤ 0.01	--	60%	2.1	1.6	40%
379-380	≤ 0.01	--	50%	1.7	0.7	50%
384-385	≤ 0.01	--	60%	2.4	3.4	30%
388-390	≤ 0.01	--	60%	1.4	0.98	30%
391-392	1.3	1.8	100%			
393-395	≤ 0.01	--	25%	1.8	1.8	75%

nts	C_m, 1	n, 1	amp 1	C_m, 2	n, 2	amp 2
398-399	≤ 0.01	--	70%	1.6	2.0	30%
405-406	≤ 0.01	--	70%	1	1.6	22%
427-429	0.062	5.5	20%	1.1	2.7	80%
451-452	1.2	1.4	80%			
469	1.4	2.1	100%			
471	≤ 0.01	--	40%	1.4	1.7	40%
481-483	4.9	1.8	100%			
484-485	≤ 0.01	--	40%	1.4	1.7	60%
487-488	≤ 0.01	--	80%	2.7	1.4	20%
498	≤ 0.01	--	50%	1.3	1.6	50%
499-500	≤ 0.01	--	50%	2.5	1.3	50%
505-506	5.6	2.7	80%			
521-522	0.49	0.72	100%			
524	0.019	1.5	30%	0.8	0.83	60%
525	0.015	1.9	33%	5.3	1.1	56%
526	0.015	2.2	45%	5.7	1.5	55%
528-531	0.04	0.86	50%	6.9	7.3	40%

Suppl. Table 1 (c) RNA plus proteins S4, S17, and S20—prot/enh/prot[e]

nt	f_{core}	C_m, 1	n, 1	C_m, N	n, N
295-297	0.55	1.4	10.4	1.7	11.4
495	0.91	0.18	2.0	1.4	4.7
496	2.0	0.13	1.8	0.75	3.3
501-502	0.61	0.35	2.0	1.8	3.5
504	0.40	1.3	2.1	5.6	4.3
513	0.88	0.18	1.8	0.39	2.2
516-518	1.8	1.7	6.9	2.5	8.3
533-536	0.44	0.33	2.2	0.96	3.1

[e]Nucleotides protected in 0.01 mM $MgCl_2$, exposed (enhanced cleavage) in 1-3 mM $MgCl_2$ and protected ≥ 3 mM $MgCl_2$ were fit to equation (1). Because I_{core} was already populated in 0.01 mM $MgCl_2$, the statistical weight of this term was treated as a constant, f_{core}.

Suppl. Table 1 (d) RNA plus protein S4, S16, S17, and S20

nts	C_m, 1	n, 1	amp 1	C_m, 2	n, 2	amp 2
59-65	1.3	1.2	66%			
66-72	0.24	2.1	66%			
100-105	0.007	0.14	50%			
107-108	3.8	0.48	70%			
110-114	0.38	0.84	70%			
115-116	0.20	0.99	70%			
119	0.39	0.78	83%			
121-124	0.28	1.6	65%			
131-133	≤ 0.01	--	65%	0.8	0.79	20%
134-135	0.13	0.86	72%			
142-143	≤ 0.01	--	30%	0.18	0.87	50%
151-153	≤ 0.01	--	30%	0.28	0.91	55%
173-174	≤ 0.01	--	60%	0.71	1.1	40%
184	≤ 0.01	--	60%	0.51	0.78	40%
196-200	≤ 0.01	--	50%	0.82	1.1	50%
203-204	≤ 0.01	--	60%	0.48	1.16	40%
210	≤ 0.01	--	70%	0.47	0.9	30%
217	≤ 0.01	--	60%	1.2	5.9	40%
219-224	≤ 0.01	--	60%	0.85	0.88	40%
250-254	≤ 0.01	--	45%	3.1	1.6	55%
263	≤ 0.01	--	60%	1.2	0.58	40%
266	≤ 0.01	--	60%	1.4	0.59	40%
276	≤ 0.01	--	60%	1.3	0.72	40%
278-280	≤ 0.01	--	80%			
282-283	≤ 0.01	--	60%	1.5	0.69	40%
288-290	0.26	0.42	100%			
295-297	≤ 0.01	--	50%	1.2	0.61	50%
301	≤ 0.01	--	40%	0.45	0.44	60%
305-307	≤ 0.01	--	40%	1.2	0.69	60%
312	0.36	0.5	100%			
315	0.06	0.33	100%			
319-322	0.67	0.72	100%			
327-330	0.54	1.2	100%			
343	1.0	0.69	100%			
348	≤ 0.01	--	60%	0.98	0.89	40%
352-357	0.81	1.0	100%			
364	1.2	0.8	60%			
370-374	0.96	0.96	100%			
378	0.49	0.99	100%			
379-380	0.61	1.1	100%			
384-385	0.36	0.6	100%			
388-390	0.32	0.84	80%			
391-392	0.54	0.83	100%			

nts	C_m, 1	n, 1	amp 1	C_m, 2	n, 2	amp 2
393-395	0.5	0.59	100%			
398-399	1.5	1.5	90%			
405-406	0.17	0.81	70%			
427-429	≤ 0.01	--	40%	2.3	4.2	40%
451-452	≤ 0.01	--	40%	2.3	3.1	55%
469	2.1	2.0	100%			
471	2.3	2.0	100%			
481-483	≤ 0.01	--	40%	2.4	3.6	60%
484-485	≤ 0.01	--	40%	2.9	17	60%
487-488	≤ 0.01	--	50%	2.8	3.1	50%
495-496	≤ 0.01	--	35%	2.9	4.1	65%
498	≤ 0.01	--	50%	2.2	3.4	50%
499-500	≤ 0.01	--	50%	2.5	3.7	50%
501-502	2.6	3.0	80%			
504	≤ 0.01	--	20%	2.5	3.0	60%
505-506	≤ 0.01	--	30%	2.3	3.8	60%
513	5.3	1.3	100%			
516-518	≤ 0.01	--	40%	7.4	1.6	60%
521-522	0.6	1.5	100%			
524-527	1.4	1.1	100%			
528-531	≤ 0.01	--	20%	2.1	1.5	70%
533-536	2.4	3.8	90%			

Supplemental Notes

1. Stern, S., Changchien, L.M., Craven, G.R. & Noller, H.F. Interaction of proteins S16, S17 and S20 with 16 S ribosomal RNA. *J. Mol. Biol.* **200**, 291-9 (1988).
2. Wimberly, B.T. et al. Structure of the 30S ribosomal subunit. *Nature* **407**, 327-339 (2000).
3. Schluenzen, F. et al. Structure of functionally activated small ribosomal subunit at 3.3 angstroms resolution. *Cell* **102**, 615-623 (2000).
4. Schuwirth, B.S. et al. Structures of the bacterial ribosome at 3.5 A resolution. *Science* **310**, 827-34 (2005).
5. Powers, T. & Noller, H.F. Hydroxyl radical footprinting of ribosomal proteins on 16S rRNA. *RNA* **1**, 194-209 (1995).
6. Brodersen, D.E., Clemons, W.M., Jr., Carter, A.P., Wimberly, B.T. & Ramakrishnan, V. Crystal structure of the 30 S ribosomal subunit from Thermus thermophilus: structure of the proteins and their interactions with 16 S RNA. *J. Mol. Biol.* **316**, 725-68 (2002).